Inorg. Chem. **2006**, *45*, 6370–6377

The HETTAP Approach: Self-Assembly and Metal Ion Sensing of Dumbbell-Shaped Molecules and Clip Molecules

Michael Schmittel,*,‡ Venkateshwarlu Kalsani,‡ Prasenjit Mal,‡ and Jan W. Bats†

Center of Micro and Nanochemistry and Engineering, Organische Chemie I, Universität Siegen, Adolf-Reichwein-Strasse 2, D-57068 Siegen, Germany, Institut für Organische Chemie und Chemische Biologie, Johann Wolfgang Goethe-Universität, Marie-Curie-Strasse 11, D-60439 Frankfurt am Main, Germany

Received March 9, 2006

The pentacoordinated terpyridine–phenanthroline zinc(II) complex motif, conceived along the HETTAP concept, allows the preparation of a set of multicomponent supramolecular dumbbell and clip assemblies from various bisterpyridines. All assemblies show a notable luminescence at 350–400 nm. The formation of dumbbell $[Zn_2(\mathbf{1b})_2(\mathbf{2b})]^{4+}$ is convincingly demonstrated from the X-ray crystal structure analysis. Both dumbbell $[Zn_2(\mathbf{1b})_2(\mathbf{2b})]^{4+}$ and clip $[Zn_2(\mathbf{1d})(\mathbf{2b})]^{4+}$ allow the monitoring of Hg^{2+} ions due to highly selective quenching of the emission that is driven by a $Zn^{2+} \rightarrow Hg^{2+}$ exchange process, while the more-strained clip $[Zn_2(\mathbf{1d})(\mathbf{2c})]^{4+}$ does not undergo such metal exchange and does not show quenching of the luminescence. Consequently, these assemblies exhibit a highly selective response due solely to supramolecular effects.

Introduction

Enticing research endeavors by Lehn,[1] Sauvage,[2] and others[3] have led to the fabrication of dynamic metallosupramolecular aggregates by relying solely on maximum site occupancy and/or ring constraints. However, due to inherent constraints, their approach does not open a general venue to heteroleptic architectures. Inspired by our recent success with the *het*eroleptic *phen*anthroline (HETPHEN)[4] complexation approach that has been used to prepare a whole range of heteroleptic nanoladders, nanoboxes, nanogrids, nanoracks, and even supramolecular basket compounds,[5] we have systematically explored the possibility of using sterically shielded 2,9-diarylphenanthrolines[6] also in combination with tridentate ligands (terpyridine building blocks) and metal ions, such as Zn^{2+} and Hg^{2+}.[7] This has recently resulted in

Chart 1. Typical Examples of (a) HETPHEN and (b) HETTAP Complexes

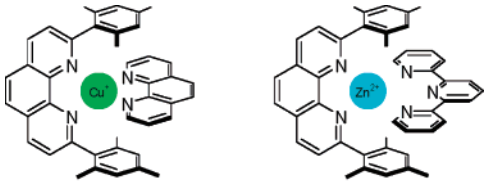

* To whom correspondence should be addressed. E-mail: schmittel@chemie.uni-siegen.de. Fax: (+49) 271 740 3270.
‡ Center of Micro and Nanochemistry and Engineering.
† Johann Wolfgang Goethe-Universität.

(1) (a) Nitschke, J. R.; Lehn, J.-M. *Proc. Natl. Acad. Sci. U.S.A.* **2003**, *100*, 11970−11974. (b) Barboiu, M.; Vaughan, G.; Graff, R.; Lehn, J.-M. *J. Am. Chem. Soc*. **2003**, *125*, 10257−10265.
(2) Hamann, C.; Kern, J.-M.; Sauvage, J.-P. *Inorg. Chem.* **2003**, *42*, 1877−1883. Champin, B.; Sartor, V.; Sauvage, J.-P. *New J. Chem.* **2006**, *30*, 22−25.
(3) (a) Schmittel, M.; Kalsani, V. *Top. Curr. Chem.* **2004**, *245*, 1−53 and refences cited therein. (b) Reid, H. O. N.; Kahwa, I. A.; White, A. J. P.; Williams, D. J. *Chem. Commun.* **1999**, 1565−1566. (c) Shinkai, S.; Ikeda, M.; Sugasaki, A.; Takeuchi, M. *Acc. Chem. Res.* **2001**, *34*, 494−503. (d) Seidel, S. R.; Stang, P. J. *Acc. Chem. Res*. **2002**, *35*, 972−983. (e) Park, S. J.; Shin, D. M.; Sakamoto, S.; Yamaguchi, K.; Chung, Y. K.; Lah, M. S.; Hong, J.-I. *Chem. Eur. J.* **2005**, *11*, 235−241. (f) Fiedler, D.; Leung, D. H.; Bergman, R. G.; Raymond, K. N. *J. Am. Chem. Soc*. **2004**, *126*, 3674−3675. (g) Burchell, T. J.; Eisler, D. J.; Puddephatt, R. J. *Inorg. Chem.* **2004**, *43*, 5550−5557. (h) Hofmeier, H.; Schubert, U. S. *Chem. Soc. Rev*. **2004**, *33*, 373−399. (i) Dumitru, F.; Petit, E.; van der Lee, A.; Barboiu, M. *Eur. J. Inorg. Chem.* **2005**, 4255−4262. (k) Fujita, M.; Tominaga, M.; Hori, A.; Therrien, B. *Acc. Chem. Res.* **2005**, *38*, 369−378. (l) Barboiu, M.; Petit, E.; van der Lee, A.; Vaughan, G. *Inorg. Chem.* **2006**, *45*, 484−486.

(4) HETPHEN concept: a quantitative approach to *het*eroleptic bis*phen*anthroline metal complexes. This approach utilizes steric and electronic effects originating from bulky aryl substituents at the bisimine coordination sites to control the coordination equilibrium both kinetically and thermodynamically. (a) Schmittel, M.; Ganz, A. *Chem. Commun*. **1997**, 999−1000. (b) Schmittel, M.; Lüning, U.; Meder, M.; Ganz, A.; Michel, C.; Herderich, M. *Heterocycl. Commun*. **1997**, *3*, 493−498. (c) The same concept was also utilized by Karpishin and co-workers, see: Miller, M. T.; Gantzel, P. K.; Karpishin, T. B. *J. Am. Chem. Soc*. **1999**, *121*, 4292−4293.

10.1021/ic060403l CCC: $33.50
Published on Web 07/07/2006

Chart 2. Phenanthroline and Terpyridine Ligands Used in the Present Study

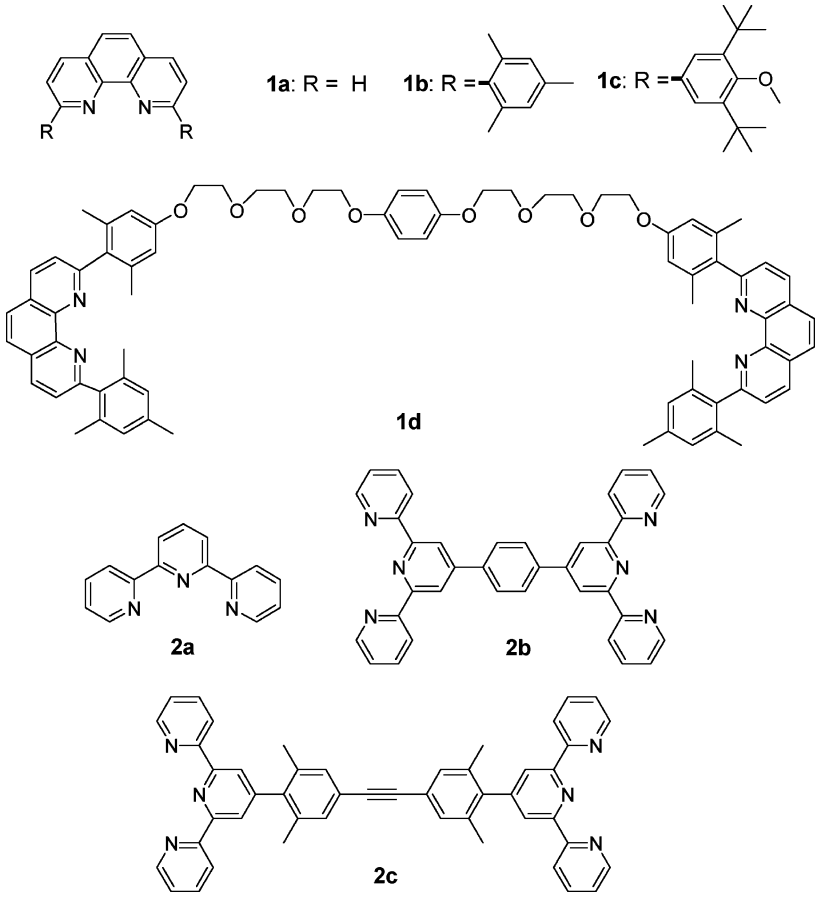

the elaboration of the HETTAP concept (*het*eroleptic *t*erpyridine *a*nd *p*henanthroline complex formation) as a tool for the construction of zinc nanoscale ladders with unique emission properties so that metal exchange processes could be monitored by the naked eye.[8] This finding is even more relevant, as there are rather few reports of utilizing Zn(II) complexes for luminescent aggregates.[9]

In the present manuscript, we describe the use of the HETTAP concept for the preparation of Zn(II)-based multicomponent dumbbell and clip structures comprised of both bisphenanthroline and tridentate (terpyridine) ligands. The ability of these assemblies to sense metal cations will also be highlighted.

Results and Discussion

Synthesis. Chart 2 depicts the phenanthroline and terpyridine building blocks used in the present study. Phenanthroline **1a** and terpyridines **2a**,**b** were purchased and used as received. Compounds **1b**−**d** were synthesized by reported procedures.[5c,6] Synthesis of **2c** (Scheme 1) was accomplished in the following manner: a condensation reaction[10] of 2,6-dimethyl-4-iodobenzaldehyde[11] and 2-acetylpyridine in the presence of KOH−NH_4OH led to the formation of 4′-(4-iodo-2,6-dimethylphenyl)-[2,2′:6′,2″]terpyridine. A subsequent Sonogashira coupling[5c] of iodoterpyridine and ethynyl trimethylsilane, followed by a deprotection reaction[12] and a subsequent Sonogashira coupling with the parent iodoterpyridine, yielded **2c**. All analytical data of **2c** were in full agreement with the suggested structure.

Heteroleptic Aggregation and Self-Assembly of Dumbbell and Clip Molecules. The essential requirement for a phenanthroline ligand to command dynamic heteroleptic aggregation is the presence of bulky alkylaryl groups in the

(5) (a) Schmittel, M.; Ammon, H.; Kalsani, V.; Michel, C.; Wiegrefe, A. *Chem. Commun.* **2002**, 2566−2567. (b) Schmittel, M.; Ganz, A.; Fenske, D. *Org. Lett.* **2003**, *4*, 2289−2292. (c) Kalsani, V.; Ammon, H.; Jäckel, F.; Rabe, J. P.; Schmittel, M. *Chem. Eur. J.* **2004**, *21*, 5481−5492. (d) Schmittel, M.; Kalsani, V.; Fenske, D.; Wiegrefe, A. *Chem. Commun.* **2004**, 490−491. (e) V. Kalsani, H. Bodenstedt, D. Fenske, M. Schmittel, *Eur. J. Inorg. Chem.* **2005**, 1841−1849. (f) Schmittel, M.; Kalsani, V.; Bats, J. W. *Inorg. Chem.* **2005**, *44*, 4115−4117.
(6) Kalsani, V.; Schmittel, M.; Listorti, A.; Accorsi, G.; Armaroli, N. *Inorg. Chem.* **2006**, *45*, 2061−2067.
(7) (a) Goodall, W.; Williams, J. A. G. *Chem. Commun.* **2001**, 2514−2515. (b) Goze, C.; Ulrich, G.; Charbonniere, L.; Cesario, M.; Prange, T.; Ziessel, R. *Chem. Eur. J.* **2003**, *9*, 3748−3755. (c) Bazzicalupi, C.; Bencini, A.; Berni, E.; Bianchi, A.; Danesi, A.; Giorgi, C.; Valtancoli, B.; Lodeiro, C.; Lima, J. C.; Pina, F.; Bernardo, M. A. *Inorg. Chem.* **2004**, *43*, 5134−5146. (d) Bazzicalupi, C.; Bencini, A.; Bianchi, A.; Danesi, A.; Giorgi, C.; Lodeiro, C.; Pina, F.; Santarelli, S.; Valtancoli, B. *Chem. Commun.* **2005**, 2630−2632. (e) Kozhevnikov, V. N.; Shabunina, O. V.; Sharifullina, A. R.; Rusinov, V. L.; Chupakhin, O. N.; König, B. *Mendeleev Commun.* **2005**, 8−9.
(8) Schmittel, M.; Kalsani, V.; Kishore, R. S. V.; Cölfen, H.; Bats, J. W. *J. Am. Chem. Soc*. **2005**, *127*, 11544−11545.
(9) Rojo, J.; Romero-Salguero, F. J.; Lehn, J.-M.; Baum, G.; Fenske, D. *Eur. J. Inorg. Chem.* **1999**, 1421−1428.
(10) Vaduvescu, S.; Potvin, P. G. *Eur. J. Inorg. Chem.* **2004**, 1763−1769.
(11) Wagner, R. W.; Johnson, T. E.; Lindsey, J. S. *J. Am. Chem. Soc*. **1996**, *118*, 11166−11180.
(12) Takase, M.; Inouye, M. *J. Org. Chem.* **2003**, *68*, 1134−1137.

Scheme 1

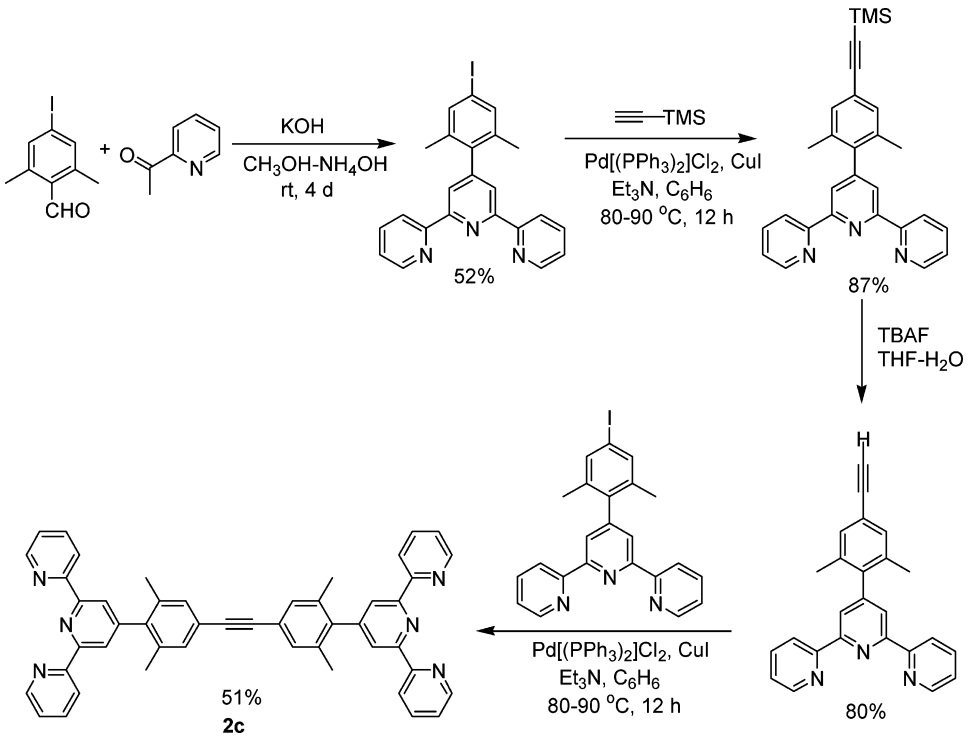

2,9 positions of the bisimine ligand. This prevents any homoleptic complex formation of these ligands in the presence of metal ions due to steric shielding. Consequently, ligands **1b**−**c** were encoded with the required control features to furnish exclusively heteroleptic assemblies. As such, their combination with metal ions such as Zn(II)[2,8] or Cu(II)[13] in the presence of **2a**−**c** is expected to yield mixed combinations preferred over homoleptic ones. If the phenanthroline ligands, however, were not encoded properly, such as **1a**, then the reaction with **2a** or **2b** yielded inseparable mixtures of dynamic homo- and heteroleptic zinc(II) aggregates, as indicated by ^{1}H NMR and ESI-MS (see Supporting Information). These results are in line with previous unsuccessful attempts to assemble bipyridine and terpyridine building blocks by Lehn and co-workers.[14] Other conditions, e.g., sequential addition and change of temperature, did not affect the composition.

No homoleptic complex could be detected by ^{1}H NMR upon reacting **1b** with zinc(II) triflate (1:10 equiv). This can easily be seen by the absence of a signal at $\delta \approx 6$ ppm, serving as a diagnostic indicator for the formation of heteroleptic and heterotopic Zn(II) complexes (see Supporting Information). Thus, ligand **1b** behaved similarly toward Zn(II) as toward Cu(I) and Ag(I) cations.[15]

Rewardingly, treatment of the molecular receptors $[Zn(\mathbf{1b},\mathbf{c})]^{2+}$ with **2a**−**c** (1:1 equiv, respectively) resulted in the quantitative formation of heteroleptic assemblies in solution, either as mononuclear complexes $[Zn(\mathbf{1b},\mathbf{c})(\mathbf{2a})]^{2+}$ or binuclear dumbbell structures $[Zn_2(\mathbf{1b},\mathbf{c})_2(\mathbf{2b})]^{4+}$ and $[Zn_2(\mathbf{1b})_2(\mathbf{2c})]^{4+}$, as clearly proven by ^{1}H NMR and ESI-MS. All compounds displayed a sharp and single set of signals in the ^{1}H NMR. The chemical shifts of the mesityl protons ($\delta \approx 7.0$ ppm in the ligand, $\delta \approx 6.2$ ppm in the complex) were most diagnostic to establish the formation of the heteroleptic complexes. In addition, the observed ^{1}H, ^{13}C NMR and ESI-MS data were all consistent with the formation of single heteroleptic assemblies. All signals in the ESI-MS were isotopically well resolved, as shown in Figure 1 for a representative example, i.e., $[Zn_2(\mathbf{1c})_2(\mathbf{2b})(OTf)]^{3+}$ and $[Zn_2(\mathbf{1c})_2(\mathbf{2b})(OTf)_2]^{2+}$.

Furthermore, the dumbbell structure of $[Zn_2(\mathbf{1b})_2(\mathbf{2b})]^{4+}$ was unequivocally established from a single-crystal measurement (Figure 2). The distance between the two Zn atoms in the dumbbell is ~1.5 nm, while the complete diameter of the dumbbell is 2.8 nm (including van der Waals radii) (Figure 2). The structure is centrosymmetric with an inversion center at the midpoint of the central benzene ring. This is one of the very few structurally characterized *nano*-dumbbells[16] and the first example of a dumbbell-shaped mixed aggregate composed of phenanthroline and terpyridine building blocks.

Cliplike[17] molecules have attracted considerable interest due to their rich host−guest chemistry.[18] As shown in Figure 3, a clip-shaped molecule is expected when **1d** and **2b**,**c** are

(13) Hasenknopf, B.; Lehn, J.-M.; Baum, G.; Fenske, D. *Proc. Natl. Acad. Sci. U.S.A.* **1996**, *93*, 1397−1400.
(14) Baxter, P. N. W.; Khoury, R. G.; Lehn, J.-M.; Baum, G.; Fenske, D. *Chem. Eur. J.* **2000**, *6*, 4140−4148.
(15) Schmittel, M.; Ganz, A.; Fenske, D.; Herderich, M. *J. Chem. Soc., Dalton Trans.* **2000**, 353−359.
(16) (a) Lu, M.; Wie, Y.; Xu, B.; Cheung, C. F.-C.; Peng, Z.; Powell, D. R. *Angew. Chem., Int. Ed.* **2002**, *41*, 1566−1568. (b) Fan, J.; Sun, W.-Y.; Okamura, T.-A.; Xie, J.; Tang, W.-X.; Ueyama, N. *New. J. Chem.* **2002**, 199−201. (c) Lukin, O.; Recker, J.; Böhmer, A.; Müller, W. M.; Kubota, T.; Okamoto, Y.; Nieger, M.; Fröhlich, R.; Vögtle, F. *Angew. Chem., Int. Ed.* **2003**, *42*, 442−445.
(17) Elemans, J. A. A. W.; Claase, M. B.; Aarts, P. P. M.; Rowan, A. E.; Schenning, A. P. H. J.; Nolte, J. M. *J. Org. Chem.* **1999**, *64*, 7009−7016.

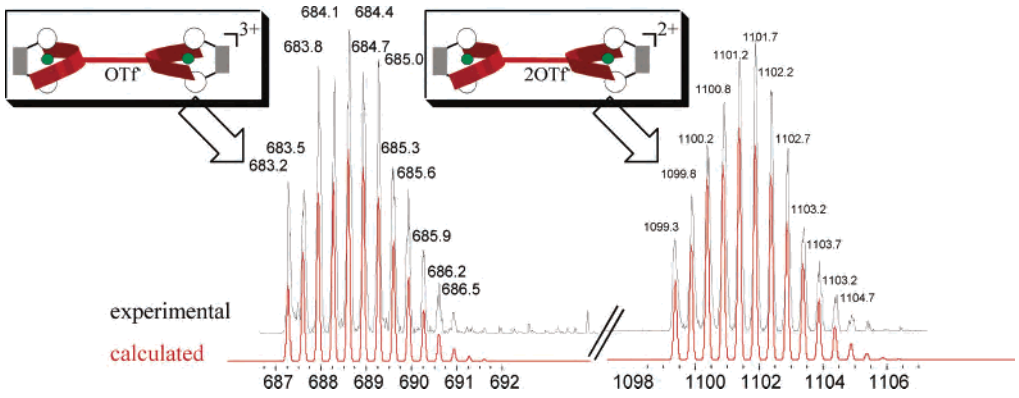

Figure 1. Isotopic distributions (red: calculated, dark: experimental) of $[Zn_2(\mathbf{1c})_2(\mathbf{2b})(OTf)]^{3+}$ (left) and $[Zn_2(\mathbf{1c})_2(\mathbf{2b})(OTf)_2]^{2+}$ (right).

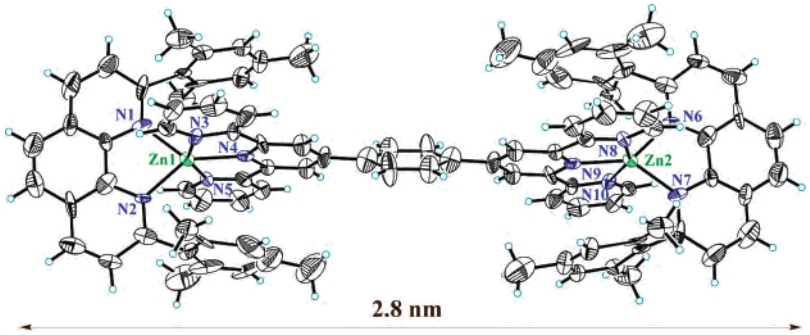

Figure 2. Solid-state molecular structure of $[Zn_2(\mathbf{1b})_2(\mathbf{2b})]^{4+}$ with displacement ellipsoids at the 50% probability level.

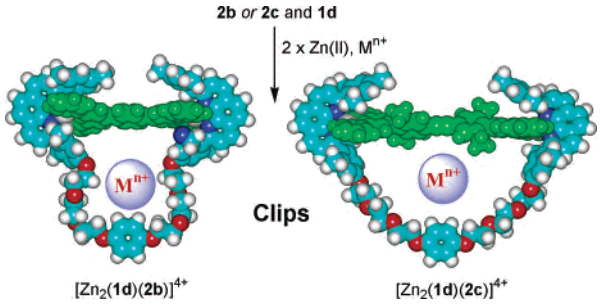

Figure 3. Self-assembly of the heteroleptic clip molecules and their potential to function as a host for metal cations: The clips are represented as a space-filling model obtained by HyperChem.

reacted with Zn(II) salt. Due to the oligoether subunit, whose conformation and flexibility may be controlled by the length of the spacer **2b** vs. **2c**, the designed clip molecules may show some suitability as chemosensors for metal cations.[19]

Upon mixing **2b**,**c** with **1d** and $[Zn(OTf)_2]$ (1:1:2) in dichloromethane (DCM)/methanol (8:2) the solution turned to a light-orange color. Analysis of this solution by ESI-MS indicated the formation of clip complexes $[Zn_2(\mathbf{1d})(\mathbf{2b},\mathbf{c})]^{4+}$ as exclusive species. The isotopic splitting clearly showed a doubly charged species being in perfect agreement with its proposed composition (see Supporting Information). The ^1H NMR spectrum showed a sharp and single set of signals, ruling out the presence of any additional aggregates. The formation of the heteroleptic aggregate was clearly ascertained by the emergence of the characteristically high-field-shifted aromatic protons (of the mesityl and dimethylphenoxy unit) at about $\delta \approx 6.0$ ppm.[5c]

Binding constants[8] for dumbbells $[Zn_2(\mathbf{1b})_2(\mathbf{2b},\mathbf{c})]^{4+}$ and the clips $[Zn_2(\mathbf{1d})(\mathbf{2b},\mathbf{c})]^{4+}$ were determined by UV−vis titration and analyzed by SPECFIT[20] (see Table 2). These values can be compared with that determined for $[Zn(\mathbf{1e})(\mathbf{2a})]^{2+}$.[8] Clearly, the determined binding constants ($\log \beta_1$ and $\log \beta$) for both the dumbbells and clips are in line with an earlier value for the Zn(II) terpyridine−phenanthroline complex.[8] As expected, $\log \beta_1$ are somewhat larger than $\log \beta_2$ values due to the reduced donor qualities of ligand **2b**,**c** when it is already coordinated to a Zn^{2+} ion. This is recognized both in dumbbells and clips.

The absorption and luminescence spectra of all ligands (**1b**,**c**; **2a**−**c**) and their complexes were recorded in a mixture of DCM/methanol (8:2) at room temperature. As shown in Figure 5, ligands **1b**,**c** and **2a**,**b** and their complexes display intense and well-resolved absorption peaks at ∼290−330 nm that can be assigned to essentially unshifted $\pi-\pi^*$ bands of the phenanthroline subunits and phenyl rings.[21] A bathochromic shift is observed for the Zn(II) complexes with respect to the ligands (Table 3), indicating increased π conjugation.[21] In contrast to the absorption behavior, Zn complexes of **1b**,**c** with **2a** exhibited an emission that was

(18) Klärner, F.-G.; Kahlert, B.; Nellesen, A.; Zienau, J.; Ochsenfeld, C.; Schrader, T. *J. Am. Chem. Soc.* **2006**, *128*, 4831−4841 and references therein.

(19) (a) Gokel, G. W.; Leevy, W. M.; Weber, M. E. *Chem. Rev.* **2004**, *104*, 2723−2750. (b) Liu, Y.; Duan, Z.-Y.; Zhang, H.-Y.; Jiang, X.-L.; Han, J.-R. *J. Org. Chem.* **2005**, *70*, 1450−1455.

(20) (a) Gampp, H.; Maeder, M.; Meyer, C. J.; Zuberbühler, A. D. *Talanta* **1985**, *32*, 95−101. (b) Rossoti, F. J. C.; Rossoti, H. S.; Whewell, R. J. *J. Inorg. Nucl. Chem.* **1971**, *33*, 2051−2065. (c) Gampp, H.; Maeder, M.; Meyer, C. J.; Zuberbühler, A. D. *Talanta* **1985**, *32*, 257−264. (d) Gampp, H.; Maeder, M.; Meyer, C. J.; Zuberbühler, A. D. *Talanta* **1986**, *33*, 943−951.

(21) Goeb, S.; Nicola, A. D.; Ziessel, R. *J. Org. Chem.* **2005**, *70*, 6802−6808.

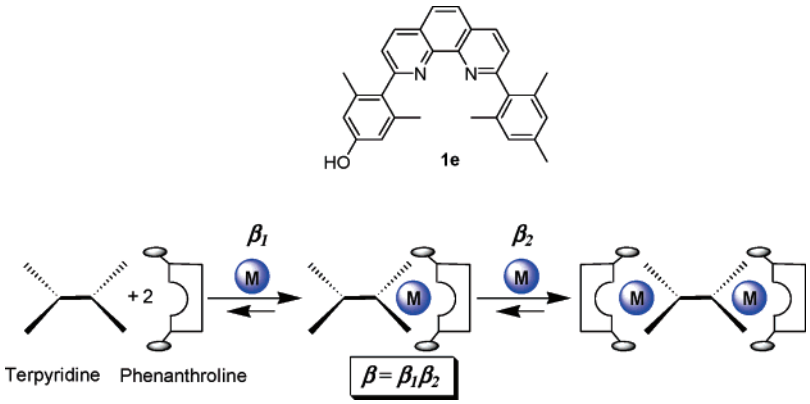

Figure 4. Cartoon representation of the stepwise formation of the dumbbell complexes.

Table 1. Selected Crystallographic Data for the Dumbbell $[Zn_2(\mathbf{1b})_2(\mathbf{2b})](OTf)_4$

substance	$[Zn_2(\mathbf{1b})_2(\mathbf{2b})](OTf)_4$
molecular formula	$C_{100}H_{80}F_{12}N_{10}O_{12}S_4Zn_2$
fw/g·mol^{-1}	2100.79
T/K	156(2)
λ/pm	71.073
cryst syst, space group	triclinic, $P\bar{1}$
unit cell dimens	a = 11.521 (2) Å
	b = 17.185 (4) Å
	c = 18.164 (4) Å
	α = 114.937(12)°
	β = 94.469 (19)°
	γ =105.15(2)°
V/Å^3	3074.0 (11)
Z, calcd density/Mg·m^{-3}	1, 1.135
absorption coefficient/mm^{-1}	0.529
F(000)	1078
cryst size/mm^3	0.36 × 0.32 × 0.10
reflns collected/unique/R_{int}	30 425/11 341/0.1577
refinement method	full-matrix least-squares on F^2
data/restraints/params	11 341/4/637
GOF on F^2	0.988
final R indices [$I > 2\sigma(I)$]	R1 = 0.1166, wR2 = 0.2564
R indices (all data)	R1 = 0.2382, wR2 = 0.2930
largest diff. peak and hole	1.069 and −0.690 e/Å^3

Table 2. Binding Constants[a] for Dumbbells $[Zn_2(\mathbf{1b})_2(\mathbf{2b},\mathbf{c})]^{4+}$ and Clips $[Zn_2(\mathbf{1d})(\mathbf{2b},\mathbf{c})]^{4+}$

entry	complex	log β_1	log β_2	log β
1	$[Zn(\mathbf{1e})(\mathbf{2a})]^{2+}$	12.4[b]	–	–
2	dumbbell $[Zn_2(\mathbf{1b})_2(\mathbf{2b})]^{4+}$	13.7 ± 0.4	12.5	26.2 ± 0.6
3	dumbbell $[Zn_2(\mathbf{1b})_2(\mathbf{2c})]^{4+}$	12.7 ± 0.5	10.6	23.3 ± 0.8
4	clip $[Zn_2(\mathbf{1d})(\mathbf{2b})]^{4+}$	13.3 ± 0.4	12.0	25.3 ± 0.6
5	clip $[Zn_2(\mathbf{1d})(\mathbf{2c})]^{4+}$	13.5 ± 0.4	12.5	26.0 ± 0.6

[a] The solvent used for all the measurements was dichloromethane/methanol (8:2). [b] See ref 8.

slightly hypsochromically shifted while those with **2b** (dumbbell structures) were red-shifted. Emission of the complexes is ascribed to fluorescence from the lowest ligand-centered (LC) excited singlet level.[9] The intense luminescence makes these assemblies attractive candidates for supramolecular sensors.

Metal Ion Sensing of the Clip Assemblies. The ability of clip $[Zn_2(\mathbf{1d})(\mathbf{2b})]^{4+}$ to act as a host for various metal cations was probed using UV−vis and luminescence spectroscopy. As can be seen from Figure 6, the emission intensity and emission wavelength of $[Zn_2(\mathbf{1d})(\mathbf{2b})]^{4+}$ in acetonitrile changed when an excess (10 equiv) of metal cations was added (e.g., Pb^{2+}, Hg^{2+}). Within the small series

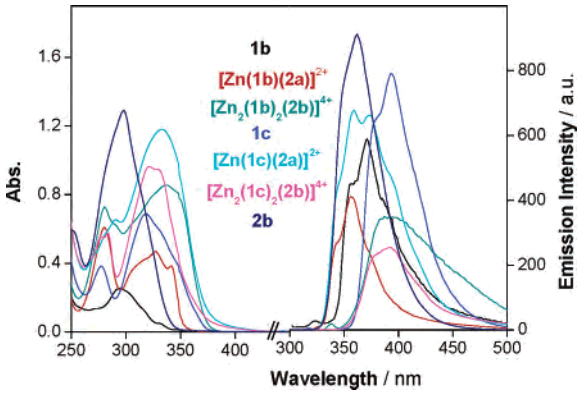

Figure 5. Absorption (left) and emission (right) spectra of **1b**,**c**, **2b**, and Zn(II) complexes of **1b**,**c** with **2a**,**b** in dichloromethane/methanol (8:2) (2.04 × 10^{-5} M).

Table 3. Absorption, Emission Intensities, and λ_{max} of the Substrates **1b**,**c**, **2b**, and Zn(II) Complexes of **1b**,**c** with **2a**,**b** in Dichloromethane/Methanol (8:2) (2.04 × 10^{-5} M)

entry	substrate	λ_{max} (abs) (nm)	ϵ_{abs} (M^{-1} cm^{-1})	λ_{max} (em)	I_{em} (au)
1	**1b**	294	12500	371	588.9
2	$[Zn(\mathbf{1b})(\mathbf{2a})]^{2+}$	280	29800	356	411.6
		327	23000		
3	$[Zn_2(\mathbf{1b})_2(\mathbf{2b})]^{4+}$	337	41900	387	350.0
4	**1c**	318	33700	393	791.1
5	$[Zn(\mathbf{1c})(\mathbf{2a})]^{2+}$	321	47200	359	677.0
		329 (sh)	46400	374	662.1
6	$[Zn(\mathbf{1c})_2(\mathbf{2b})]^{4+}$	333	57900	393	255.3
7	**2b**	298	63200	362	912.0

of cations studied, the strongest luminescence increase was observed upon addition of Pb^{2+} ions (50% with respect to $[Zn_2(\mathbf{1d})(\mathbf{2b})]^{4+}$) (Table 4). In contrast, upon addition of Hg^{2+}, efficient luminescence quenching[22] of $[Zn_2(\mathbf{1d})(\mathbf{2b})]^{4+}$ was noticed, as depicted in Figure 6. Noticeably, an analogous luminescence decrease was equally observed when dumbbell $[Zn_2(\mathbf{1b})_2(\mathbf{2b})]^{4+}$), containing no oligoether tether, was treated with Hg^{2+} ions.

As a consequence of this finding, we carefully analyzed the mixtures of clip $[Zn_2(\mathbf{1d})(\mathbf{2b})]^{4+}$ with the various metal ions under investigation. Upon addition of Na^+, K^+, Mg^{2+}, Ca^{2+}, Pb^{2+}, and Ba^{2+} ESI-MS data confirmed the structural integrity of $[Zn_2(\mathbf{1d})(\mathbf{2b})]^{4+}$. In contrast, a mixture of $[Zn_2(\mathbf{1d})(\mathbf{2b})]^{4+}$ + $n$$Hg^{2+}$] furnished isotopically well-resolved

(22) Métivier, R.; Leray, I.; Valeur, B. *Chem. Eur. J.* **2004**, *10*, 4480−4490.

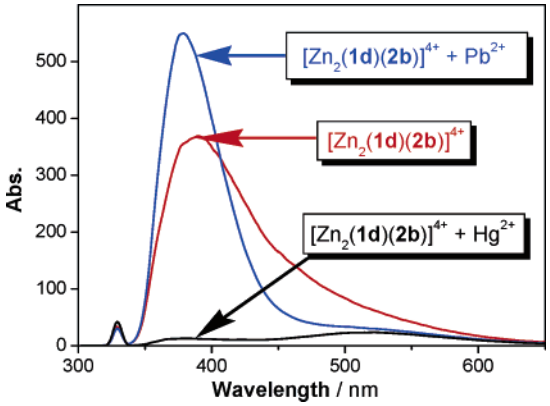

Figure 6. Luminescence spectra of clip $[Zn_2(\mathbf{1d})(\mathbf{2b})]^{4+}$ at 2.04×10^{-5} M in the presence of Pb^{2+}, Hg^{2+} in acetonitrile at room temperature (metal salts used as their perchlorate salts; 10 equiv of each metal ion was added). Excitation wavelength: 330 nm.

Table 4. Relative Emission Intensities and λ_{max} (em) of the Clip $[Zn_2(\mathbf{1d})(\mathbf{2b})]^{4+}$ without and in the Presence of Different Metal Ions at 2.04×10^{-5} M in Acetonitrile at Room Temperature[a]

entry	substrate	λ_{max} (em) (nm)	I_{em} (corr) (au)	$I/I_{(clip)}$
1	$[Zn_2(\mathbf{1d})(\mathbf{2b})]^{4+}$	390	369.1	–
2	$[Zn_2(\mathbf{1d})(\mathbf{2b})]^{4+} + Na^+$	387	372.0	1.01
3	$[Zn_2(\mathbf{1d})(\mathbf{2b})]^{4+} + K^+$	381	482.8	1.31
4	$[Zn_2(\mathbf{1d})(\mathbf{2b})]^{4+} + Mg^{2+}$	373	572.5	1.55
5	$[Zn_2(\mathbf{1d})(\mathbf{2b})]^{4+} + Ca^{2+}$	376	489.8	1.33
6	$[Zn_2(\mathbf{1d})(\mathbf{2b})]^{4+} + Ba^{2+}$	375	355.6	0.96
7	$[Zn_2(\mathbf{1d})(\mathbf{2b})]^{4+} + Pb^{2+}$	379	549.9	1.49
8	$[Zn_2(\mathbf{1d})(\mathbf{2b})]^{4+} + Hg^{2+}$	381	12.9	0.03

[a] Metal salts used as their perchlorate salts; 10 equiv of each metal ion was added. Excitation wavelength: 330 nm.

signals corresponding to the Hg-clip $[Hg_2(\mathbf{1d})(\mathbf{2b})]^{4+}$. Signals of $[Zn_2(\mathbf{1d})(\mathbf{2b})]^{4+}$ decreased with time, disappearing completely within ca. 3−4 h (see Supporting Information), indicative of full exchange of Zn^{2+} ions in $[Zn_2(\mathbf{1d})(\mathbf{2b})]^{4+}$ by Hg^{2+} ions. However, the time scale of ion exchange has to be compared with the time scale of luminescence quenching. For clip $[Zn_2(\mathbf{1d})(\mathbf{2b})]^{4+}$, the luminescence quenching was completed in ca. 10 min (see Supporting Information). On this time scale, Zn^{2+} ions in the clip were only partly replaced by Hg^{2+}, as established by ESI-MS and ^{1}H NMR evidence.

To gain further insight, we determined the change in the luminescence intensity of clip $[Zn_2(\mathbf{1d})(\mathbf{2b})]^{4+}$ upon addition of just 1 equiv of Hg^{2+} salt. At this ratio, the luminescence did not decrease but instead increased by 20−30% (see Supporting Information), reaching a constant augmented emission after ca. 10 min. ESI-MS analysis of this mixtures established that the clip $[Zn_2(\mathbf{1d})(\mathbf{2b})]^{4+}$ was unaffected by ion exchange, and ^{1}H NMR showed only Hg^{2+}-induced shifts of diagnostic signals of the oligoether chain (in CD_3CN, 400 MHz, see Supporting Information).

As a further control experiment to assess the role of the oligoether chain, we investigated the luminescence behavior of the dumbbell $[Zn_2(\mathbf{1b})_2(\mathbf{2b})]^{4+}$ in the presence of Pb^{2+} and Hg^{2+} ions in acetonitrile. The insubstantial decrease in the luminescence intensity observed upon addition of 1.0 equiv of the metal ions as perchlorate salts clearly demonstrates that the metal ions do not enhance luminescence without coordination to the oligoether tether.

The combined data suggest that upon addition of Hg^{2+} ions to $[Zn_2(\mathbf{1d})(\mathbf{2b})]^{4+}$ there is at first an association of the metal ions with the oligoether tether that leads to an increase in the luminescence as observed equally for Na^+, K^+, Mg^{2+}, Ca^{2+}, Pb^{2+}, and Ba^{2+}. Association of the metal ions, e.g. for Hg^{2+} and Pb^{2+}, for the oligoether tether is indeed corroborated by ^{1}H NMR results (see Supporting Information). Hence, the luminescence increase is mostly due to a complexation of the metal ions to the oxygen atoms and hydroquinone unit of the tether, thus diminishing the donor character of these subunits that are known to be involved in luminescence quenching by electron transfer. If Hg^{2+} ions are added in large excess, a slow Zn^{2+}/Hg^{2+} exchange process follows, leading to the formation of $[ZnHg(\mathbf{1d})(\mathbf{2b})]^{4+}$ and $[Hg_2(\mathbf{1d})(\mathbf{2b})]^{4+}$. As the luminescence quenching (at 10 equiv of Hg^{2+} ions) is much faster than formation of $[Hg_2(\mathbf{1d})(\mathbf{2b})]^{4+}$, we suggest that already the formation of $[ZnHg(\mathbf{1d})(\mathbf{2b})]^{4+}$ is sufficient to quench emission in the clip assembly.

On the other hand, when clip $[Zn_2(\mathbf{1d})(\mathbf{2b})]^{4+}$ was replaced by clip $[Zn_2(\mathbf{1d})(\mathbf{2c})]^{4+}$, analogous quenching or enhancement of luminescence was not observed upon addition of the respective metal ions, both in DCM/methanol (8:2) and in acetonitrile. ESI-MS analysis of the mixture $[Zn_2(\mathbf{1d})(\mathbf{2c})]^{4+} + n Hg^{2+}]$ did not provide any information for the formation of the Hg-clip $[Hg_2(\mathbf{1d})(\mathbf{2c})]^{4+}$, even after 24 h in the presence of ∼10 equiv of the Hg^{2+} salt. Force field calculations on $[Zn_2(\mathbf{1d})(\mathbf{2c})]^{4+}$ (Figure 3) suggest that the oligoether tether in $[Zn_2(\mathbf{1d})(\mathbf{2c})]^{4+}$ is much more locked and strained than in $[Zn_2(\mathbf{1d})(\mathbf{2b})]^{4+}$. This has two effects: due to the strain, (i) the oligoether chain can apparently not wrap around the metal ion thus precluding efficient complexation, and (ii) the dissociation of the coordinating metal ion is slowed, explaining the inability of $[Zn_2(\mathbf{1d})(\mathbf{2c})]^{4+}$ to exchange Zn^{2+} ions by Hg^{2+} ions.

Conclusions

In summary, a novel, general, and facile approach to supramolecular dumbbell and clip-shaped aggregates is presented on the basis of the HETTAP approach. Because the resulting aggregates are luminescent, ready access to novel photophysically active architectures is provided. Clip $[Zn_2(\mathbf{1d})(\mathbf{2b})]^{4+}$ shows a noticeable luminescence enhance-

Figure 7. Metal ion sensing of the clip $[Zn_2(\mathbf{1d})(\mathbf{2b})]^{4+}$ assembly.

ment after addition of Pb^{2+}. Both the clip and the heteroleptic dumbbell $[Zn_2(\mathbf{1b})_2(\mathbf{2b})]^{4+}$ exhibit luminescence quenching upon addition of Hg^{2+} ions. The quenching after addition of Hg^{2+} is driven by a metal-exchange mechanism in the dumbbell and clip $[Zn_2(\mathbf{1d})(\mathbf{2b})]^{4+}$, which cannot occur in clip $[Zn_2(\mathbf{1d})(\mathbf{2c})]^{4+}$ due to slow dissociation kinetics. Luminescence quenching is believed to be due to an electron-transfer process from the fluorophore to the metal center.

Experimental Section

Phenanthroline building blocks **1b**−**d** were prepared by known procedures. Terpyridine building blocks **2a**,**b** were purchased from Aldrich and used as received. Terpyridine **2c** was prepared by following a known literature procedure. ^{1}H and ^{13}C NMR were measured on Bruker AC 200 (200 MHz) and Bruker Avance 400 (400 MHz) spectrometers. ESI-MS spectra were measured on a LCQ Deca Thermo Quest instrument. Typically, each time 25 scans were accumulated for one spectrum. All complexes were characterized by ^{1}H, ^{13}C, and ESI-MS analysis. UV−visible spectra were recorded on a Varian Cary 100 Bio UV−visible spectrometer and Varian Cary Eclipse fluorescence spectrometer.

Sythesis of Bis[(4′-(2,6-dimethylphenyl)-(2,2′:6′,2″)terpyridyl]-acetylene (2c). Synthesis of 4′-(4-Iodo-2,6-dimethylphenyl)-[2,2′,6′,2″]terpyridine. 2-Acetylpyridine (4.84 g, 40.0 mmol) was added to a solution of 2,6-dimethyl-4-iodobenzaldehyde (5.08 g, 20.0 mmol) in 100.0 mL of methanol. 15% aq KOH (15.0 mL) and concentrated NH_4OH (100.0 mL) were then added to the solution, and vigorous stirring was maintained for 4 days. The light-yellow precipitate that formed was collected by filtration, washed thoroughly with water, and on recrystallization from methanol/DCM (20:1) yielded 1.47 g (52% on 30% conversion) of 4′-(4-iodo-2,6-dimethylphenyl)-[2,2′,6′,2″]terpyridine as a colorless crystalline solid, mp 187−188 °C; ^{1}H NMR ($CDCl_3$, 200 MHz): δ 2.06 (s, 6H), 7.30−7.36 (m, 2H), 7.49 (s, 2H), 7.88 (dt, J = 7.8, 1.7 Hz, 2H), 8.30 (s, 2H), 8.66−8.72 (m, 4H); ^{13}C NMR ($CDCl_3$, 50 MHz): δ 20.4, 93.4, 121.2, 121.4, 123.9, 136.1, 136.9, 137.5, 139.2, 149.1, 150.4, 155.8, 155.9; IR (KBr): $\tilde{\nu}$ = 2921, 1601, 1586, 1568, 1541, 1467, 1386 cm^{-1}; ESI-MS: Calcd for $C_{23}H_{18}IN_3$ [M^+] (%): m/z 463.3. Found: (m + 1)/z 464.6 (100); Anal. Calcd for $C_{23}H_{18}IN_3$ C, 59.62; H, 3.92; N, 9.07. Found: C, 59.27; H, 3.72; N, 8.95.

Synthesis of 4′-(2,6-Dimethyl-4-trimethylsilanylethynylphenyl)-[2,2′:6′,2″]terpyridine. 4′-(4-Iodo-2,6-dimethylphenyl)-[2,2′:6′,2″]terpyridine (700 mg, 1.51 mmol), ethynyl trimethylsilane (300 mg, 3.02 mmol), $[Pd(PPh_3)_2]Cl_2$ (106 mg, 0.151 mmol), and CuI (144 mg, 0.151 mmol) were suspended in benzene (15 mL) and triethylamine (7.5 mL) under nitrogen. The reaction mixture was heated at 90 °C for 12 h and monitored by ESI-MS. It was then diluted with DCM (60 mL) and washed with saturated NaCl solution. The organic layer was dried over anhydrous $MgSO_4$. On evaporation of the solvent, followed by recrystallization from methanol, 571 mg (yield 87%) of a colorless solid, i.e., 4′-(2,6-dimethyl-4-trimethylsilanylethynylphenyl)-[2,2′:6′,2″]terpyridine, was obtained, mp 156−157 °C; ^{1}H NMR ($CDCl_3$, 200 MHz): δ 0.27 (s, 9H), 2.07 (s, 6H), 7.26 (s, 2H), 7.33−7.40 (m, 2H), 7.91 (dt, J = 7.7, 1.7 Hz, 2H), 8.30 (s, 2H), 8.69−8.74 (m, 4H); ^{13}C NMR ($CDCl_3$, 50 MHz): δ 0.01, 20.6, 93.8, 97.0, 105.3, 121.4, 121.6, 122.3, 124.0, 130.9, 135.4, 137.2, 149.0, 151.0, 155.5, 155.8; IR (KBr): $\tilde{\nu}$ = 2956, 2157, 1607, 1585, 1562, 1467, 1392 cm^{-1}; ESI-MS: Calcd for $C_{28}H_{27}N_3Si$ [M^+] (%): m/z 433.62. Found: (m + 1)/z 434.7 (100); Anal. Calcd for $C_{28}H_{27}N_3Si$: C, 77.56; H, 6.28; N, 9.69. Found: C, 77.17; H, 6.25; N, 9.63.

Synthesis of 4′-(4-Ethynyl-2,6-dimethylphenyl)-[2,2′:6′,2″]-terpyridine. To a THF (15.0 mL) solution of 4′-(2,6-dimethyl-4-trimethylsilanylethynylphenyl)-[2,2′:6′,2″]terpyridine (542 mg, 1.25 mmol) was added TBAF (592 mg, 1.875 mmol) and 1.0 mL of water. The reaction mixture was stirred at room temperature overnight. After removal of the solvent, DCM was added and the organic layer was washed with saturated NaCl solution and dried over anhydrous $MgSO_4$. Evaporation of the solvent followed by Silica gel column chromatography with DCM/CH_3OH (9:1) led to isolation of a colorless solid (yield 362 mg, 80%), mp 180−181 °C; ^{1}H NMR ($CDCl_3$, 200 MHz): δ 2.08 (s, 6H), 3.06 (s, 1H), 7.27 (s, 2H), 7.31−7.37 (m, 2H), 7.89 (dt, J = 7.5, 1.5 Hz, 2H), 8.30 (s, 2H), 8.68−8.72 (m, 4H); ^{13}C NMR ($CDCl_3$, 50 MHz): δ 20.6, 76.8, 83.8, 121.2, 121.3, 121.4, 123.9, 131.0, 135.6, 137.0, 140.3, 149.1, 150.8, 155.7, 156.0; IR (KBr): $\tilde{\nu}$ = 3249, 3059, 2918, 1606, 1588, 1563, 1467, 1391 cm^{-1}; ESI-MS: Calcd for $C_{25}H_{19}N_3$ [M^+] (%): m/z 361.4. Found: (m + 1)/z 362.5 (100); Anal. Calcd for $C_{25}H_{19}N_3$: C, 83.08; H, 5.30; N, 11.63. Found: C, 82.96; H, 5.26; N, 11.53.

Sythesis of Bis[4′-(2,6-dimethylphenyl)-(2,2′:6′,2″)terpyridyl]-acetylene. A Sonogashira coupling of 4′-(4-ethynyl-2,6-dimethylphenyl)-[2,2′,6′,2″]terpyridine with 4′-(4-iodo-2,6-dimethylphenyl)-[2,2′,6′,2″]terpyridine afforded bis[4′-(2,6-dimethylphenyl)−(2,2′:6′,2″)-terpyridyl]acetylene in 51% yield, mp > 300 °C; ^{1}H NMR (CD_2Cl_2, 200 MHz): δ 2.13 (s, 12H), 7.38 (s, 4H), 7.32−7.39 (m, 4H), 7.91 (dt, J = 7.8, 1.7 Hz, 4H), 8.34 (s, 4H), 8.66−8.73 (m, 8H); ^{13}C NMR ($CDCl_3$, 50 MHz): δ 20.1, 88.8, 120.7, 121.1, 122.1, 123.6, 130.2, 135.4, 136.5, 139.7, 148.9, 150.4, 155.5, 155.7; IR (KBr): $\tilde{\nu}$ = 3055, 1608, 1584, 1567, 1466, 1392 cm^{-1}; ESI-MS: Calcd for $C_{48}H_{36}N_6$ [M^+] (%): m/z 696.8. Found: (m + 1)/z 697.8 (100); Anal. Calcd for $C_{48}H_{36}N_6$: C, 82.73; H, 5.21; N, 12.06. Found C, 82.97; H, 5.17; N, 11.86.

General Procedure for the Heterotopic Assemblies. The molecular receptors [Zn(**1b**,**c**)] were prepared by reacting **1b** or **1c** (10.0 mg, 2.40 × 10^{-2} mmol or 14.8 mg 2.40 × 10^{-2} mmol, respectively) with $[Zn(OTf)_2]$ (8.72 mg, 2.40 × 10^{-2} mmol) (1:1 equiv) in a DCM/methanol mixture (8:2). The resulting solutions were analyzed without any further purification by ^{1}H NMR and used directly for the preparation of heterotopic aggregates. In all cases, no purification procedures were required for the characterization.

[Zn(1b)]$^{2+}$. ^{1}H NMR (CD_2Cl_2/CD_3OD (8:2), 200 MHz): δ 1.98 (s, 12H, benzyl), 2.32 (s, 6H, benzyl), 7.03 (s, 4H, phenyl), 7.95 (d, J = 8.37, 2H, phen), 8.28 (s, 2H, phen), 8.90 (d, J = 8.12, 2H, phen)

[Zn(1b)(2a)]$^{2+}$. ^{1}H NMR (CD_2Cl_2/CD_3OD (8:2), 200 MHz): δ 1.11 (s, 12H, benzyl), 1.78 (s, 6H, benzyl), 7.53 (t, J = 5.18 Hz, 2H, terpy), 7.70 (d, J = 4.9 Hz, 2H, terpy), 8.07 (d, J = 8.4 Hz, 2H, phen), 8.29 (t, J = 7.6 Hz, 2H, terpy), 8.51 (s, 5H, terpy), 8.56 (s, 2H, phen), 9.10 (d, J = 8.4 Hz, 2H, phen); ^{13}C NMR (CD_2Cl_2/CD_3OD (8:2), 50 MHz): 19.4 (benzyl), 20.5, 123.3 (arom), 123.6, 127.9, 128.2, 128.4, 129.6, 134.7, 135.2 (2C), 140.4, 143.2 (2C), 144.8, 146.8, 147.6, 149.2 (2C), 161.3; ESI-MS: Calcd for $[ZnC_{45}H_{39}N_5(OTf)]^+$ [M^+] (%): m/z 862.2. Found: m/z 862.1 (100), Calcd for $[ZnC_{45}H_{39}N_5]^{2+}$ [M^{2+}] (%): m/z 356.6. Found: m/z 357.2 (52).

[Zn(1c)(2a)]$^{2+}$. ^{1}H NMR (CD_2Cl_2/CD_3OD (8:2), 200 MHz): δ 0.90 (s, 36H, *t*-Bu), 3.28 (s, 6H, methoxy), 6.75 (s, 4H, phenyl), 7.71 (d, J = 4.9 Hz, 2H, terpy), 8.05 (d, J = 8.4 Hz, 2H, phen), 8.24 (t, J = 7.9 Hz, 2H, terpy), 8.45 (s, 2H, phen), 8.50 (d, J = 5.7 Hz, 3H, terpy), 8.62 (d, J = 8.8 Hz, 2H, terpy), 9.00 (d, 2H, J = 8.4 Hz, phen); ^{13}C NMR (CD_2Cl_2/CD_3OD (8:2), 50 MHz): 32.1 (*t*-Bu), 36.5, 65.9 (methoxy), 124.2 (arom.), 124.7, 126.2 (2C),

128.6, 128.9, 129.9, 130.1, 133.7 (2C), 140.7, 141.5, 143.4, 143.8, 146.4 (2C), 146.8, 147.6, 149.0, 149.4, 162.5, 162.8; ESI-MS: Calcd for $[ZnC_{57}H_{63}N_5O_2]^{2+}$ $[M^+]$ (%): *m*/*z* 456.7. Found: *m*/*z* 456.8 (100).

$[Zn_2(1b)_2(2b)]^{4+}$. ^{1}H NMR (CD_2Cl_2/CD_3OD (8:2), 200 MHz): δ 1.16 (s, 24H, benzyl), 1.79 (s, 12H, benzyl), 6.27 (s, 8H, phenyl), 7.55 (t, J = 5.4 Hz, 4H, terpy), 7.71 (d, J = 4.2 Hz, 4H, terpy), 8.10 (d, J = 8.4 Hz, 4H, phen), 8.35 (t, J = 7.9 Hz, 4H, terpy), 8.55 (s, 4H, phen), 8.59 (s, 4H, terpy), 8.94 (d, J = 8.1 Hz, 4H, terpy), 9.04 (s, 4H, phenyl), 9.10 (d, J = 8.1 Hz, 4H, phen); ^{13}C NMR (CD_2Cl_2/CD_3OD (8:2), 50 MHz): 19.5 (aliph.), 20.6, 128.8 (arom), 124.3, 128.1, 128.3, 128.4, 129.6, 129.8, 134.7, 135.3, 137.9, 140.7, 141.5, 143.2, 147.2, 148.4, 149.0, 155.9, 161.5; ESI-MS: Calcd for $[Zn_2C_{96}H_{80}N_{10}\cdot 2OTf]^{2+}$ $[M^{2+}]$ (%): *m*/*z* 901.3. Found: *m*/*z* 901.0 (100), Calcd for $[Zn_2C_{96}H_{80}N_{10}(OTf)]^{3+}$ $[M^{3+}]$ (%): *m*/*z* 551.2. Found: *m*/*z* 551.4 (45). See single-crystal structure.

$[Zn_2(1b)_2(2c)]^{4+}$. ^{1}H NMR (CD_2Cl_2/CD_3OD (8:2), 400 MHz): δ 1.23 (s, 24H, benzyl), 1.93 (s, 12H, benzyl), 2.22 (s, 12H, benzyl), 6.30 (s, 8H, phenyl), 7.50 (s, 4H, terpy), 7.58 (t, J = 5.9 Hz, 4H, terpy), 7.78 (d, J = 4.3 Hz, 4H, terpy), 8.05 (d, J = 8.3 Hz, 4H, phen), 8.30 (t, J = 6.5 Hz, 4H, terpy), 8.32 (s, 4H, terpy), 8.47 (d, J = 8.0 Hz, 4H, terpy), 8.54 (s, 4H, phen), 9.11 (d, J = 8.0 Hz, 4H, phen); ^{13}C NMR (CD_2Cl_2/CD_3OD (8:2), 100 MHz): δ 18.8 (aliph.), 20.2, 20.3, 89.2, 122.9 (arom), 123.4, 127.3 (3C), 127.7, 127.9, 128.2, 129.1, 131.0, 134.0, 134.8 (2C), 139.7, 141.0, 142.6 (2C), 145.8, 147.4, 148.7, 158.1, 160.9; ESI-MS: Calcd for $[Zn_2C_{108}H_{92}N_{10}\cdot 2OTf]^{2+}$ $[M^{2+}]$ (%): *m*/*z* 979.4. Found: *m*/*z* 979.0 (48), Calcd for $[Zn_2C_{78}H_{64}N_8(OTf)_2]^{2+}$ $[M^{2+}]$ (%): *m*/*z* 771.2. Found: *m*/*z* 771.4 (100).

$[Zn_2(1c)_2(2b)]^{4+}$. ^{1}H NMR (CD_2Cl_2/CD_3OD (8:2), 200 MHz): δ 0.96 (s, 72H, *t*-Bu), 3.28 (s, 12H, methoxy), 6.82 (s, 8H, phenyl), 7.60 (t, J = 7.4 Hz, 4H, terpy), 7.72 (d, J = 3.9 Hz, 4H, terpy), 8.10 (d, J = 8.4 Hz, 4H, phen), 8.29 (d, J = 7.9 Hz, 4H, terpy), 8.35 (s, 4H, phenyl), 8.49 (s, 4H, phen), 8.97 (d, J = 7.9 Hz, 4H, terpy), 9.05 (d, J = 8.4 Hz, 4H, phen), 9.12 (s, 4H, terpy); ^{13}C NMR (CD_2Cl_2/CD_3OD (8:2), 50 MHz): 31.4 (*t*-Bu), 35.9, 65.2 (methoxy), 124.4 (arom.), 125.6, 128.2, 129.1, 129.4, 129.8, 133.1, 137.6, 140.9, 142.7, 143.2, 145.9, 147.2, 148.4, 149.1, 156.8, 162.0, 162.3; ESI-MS: Calcd for $[ZnC_{120}H_{128}N_{10}O_4(OTf)_2]^{2+}$ $[M^{2+}]$ (%): *m*/*z* 1101.6. Found: *m*/*z* 1101.7 (100), Calcd for $[ZnC_{120}H_{128}N_{10}O_4(OTf)]^{3+}$ $[M^{3+}]$ (%): *m*/*z* 684.7. Found: *m*/*z* 684.7 (15).

$[Zn_2(1d)(2b)]^{4+}$. ^{1}H NMR (CD_2Cl_2/CD_3OD (8:2), 400 MHz): δ 1.13 (s, 12H, benzyl), 1.23 (s, 12H, benzyl), 1.68 (s, 6H, benzyl), 3.42−3.70 (m, 24H, ether), 5.99 (s, 4H, phenyl), 6.24 (s, 4H, phenyl), 6.68 (s, 4H, phenyl), 7.54 (t, J = 5.3 Hz, 4H, terpy), 7.71 (d, J = 5.8 Hz, 4H, terpy), 8.31 (t, J = 7.8 Hz, 4H, terpy), 8.41 (d, J = 8.1 Hz, 4H, phen), 8.49 (s, 8H, terpy and phenyl), 8.92 (d, J = 8.2 Hz, 4H, phen), 9.12 (s, 4H, terpy), 9.23 (d, J = 7.9 Hz, 4H, phen); ^{13}C NMR (CD_2Cl_2/CD_3OD (8:2), 100 MHz): δ 19.4 (benzyl), 20.0, 20.8, 60.6 (methoxy), 61.7, 68.1, 68.8, 70.3, 71.1, 113. 6 (arom.), 113.7, 116.1, 116.7, 119.6, 121.1, 122.7, 124.5, 128.2, 128.6, 129.0, 129.7, 129.9, 130.6, 135.1, 135.5, 137.5, 138.2, 140.8, 141.8, 143.4, 145.8, 147.5, 148.7, 149.3, 153.7, 153.8, 155.9, 160.2, 161.5, 161.7; ESI-MS: Calcd for $[Zn_2C_{112}H_{102}N_{10}O_8(OTf)_2]^{2+}$ $[M^{2+}]$ (%): *m*/*z* 1072.5. Found: *m*/*z* 1072.7 (100), Calcd for $[Zn_2C_{112}H_{102}N_{10}O_8(OTf)]^{3+}$ $[M^{3+}]$ (%): *m*/*z* 665.3. Found: *m*/*z* 665.2 (70).

$[Zn_2(1d)(2c)]^{4+}$. ^{1}H NMR (CD_2Cl_2/CD_3OD (8:2), 400 MHz): δ 1.29 (s, 24H, benzyl), 1.96 (s, 6H, benzyl), 2.23 (s, 6H, benzyl), 2.33 (s, 6H, benzyl), 3.64−3.84 (m, 24H, ether), 6.01 (s, 4H, phenyl), 6.34 (s, 4H, phenyl), 6.93 (s, 4H, phenyl), 7.49−7.62 (m, 8H, terpy, phen), 7.78 (d, J = 5.8 Hz, 4H, terpy), 8.12 (dd, J = 8.2, 3.2 Hz, 4H, terpy), 8.31 (t, J = 7.5 Hz, 4H, terpy), 8.42 (s, 4H, terpy), 8.54 (d, J = 8.1 Hz, 4H, terpy), 8.58 (s, 4H, phen), 9.15 (dd, J = 8.3, 4.0 Hz, 4H, phen); ^{13}C NMR (CD_2Cl_2/CD_3OD (8:2), 100 MHz): δ 18.8 (benzyl), 19.2, 20.1, 20.2, 67.2 (methoxy), 68.1, 69.0, 69.2, 69.4, 70.3, 89.4 (alkyne), 112.4 (arom.), 115.2, 115.6 (2C), 121.8, 123.0, 123.6, 127.3 (2C), 127.7, 127.8, 128.0, 128.2, 129.0, 130.9, 131.0, 134.8, 134.8, 135.5, 136.8, 139.7, 140.9, 141.4, 142.6 (2C), 146.0, 147.4, 147.4, 148.5, 152.8, 158.2, 159.2, 160.5, 160.9; ESI-MS: Calcd for $[Zn_2C_{124}H_{114}N_{10}O_8(OTf)_2]^{2+}$ $[M^{2+}]$ (%): *m*/*z* 1150.6. Found: *m*/*z* 1150.3 (27). Calcd for $[Zn_2C_{124}H_{114}N_{10}O_8(OTf)]^{3+}$ $[M^{3+}]$ (%): *m*/*z* 717.4 Found: *m*/*z* 717.2 (100), Calcd for $[Zn_2C_{124}H_{114}N_{10}O_8]^{4+}$ $[M^{4+}]$ (%): *m*/*z* 500.7. Found: *m*/*z* 500.7 (19).

Crystal Structure Determination of $[Zn_2(1b)_2(2b)](OTf)_4$. A single crystal (pale yellow plate with dimensions 0.10 × 0.32 × 0.36 mm^3) was measured on a SIEMENS SMART diffractometer at a temperature of 156 K. Repeatedly measured reflections remained stable. An empirical absorption correction with program SADABS[23] gave a correction factor between 0.615 and 1.000. Equivalent reflections were averaged. $R(I)_{\text{internal}}$ = 0.158. The structure was determined by direct methods using the program SIR97. The unit cell contains a solvent-accessible area of about 936 Å^3. Only a few solvate groups, probably methanol, could be seen in the solvate region. The program PLATON/SQUEEZE[24] was used to model the solvate density. The solvent electron count was estimated as about 357 electrons/cell. The H atoms were geometrically positioned and were constrained. The non-H atoms were refined with anisotropic thermal parameters. The structure was refined on F^2 values using the program SHELXL-97.[25] The final difference density was between −0.69 and +1.07 e/A^3.

Spectrophotometric Titrations. Equilibrium constants (Table 1) were calculated by using DCM/methanol (8:2) as the solvent. All stock solutions were prepared by careful weighing using an analytical balance. In a typical run, 2.0 mL of 1.02 × 10^{-5} M solution of the mixture of phenanthroline and terpyridine was taken and to it Zinc(II) triflate (2.04 × 10^{-4} M) solution was periodically added (100 μL) and spectra were recorded. Absorption spectra were recorded at 25.0(0.1) °C. Each titration consisted of ca. 20 additions. The wavelength region from 250 to 500 nm was taken into account. The entire multiwavelength data sets were decomposed in their principal components by factor analysis. Subsequently, the formation constants, including their standard deviation, were calculated using the SPECFIT program 6.[8]

Acknowledgment. We are grateful to the Deutsche Forschungsgemeinschaft, the Humboldt Foundation, and the Fonds der Chemischen Industrie for financial support. In addition, we are indebted to Prof. H. Ihmels for providing access to the Varian Cary 100 Bio UV−vis and Eclipse fluorescence spectrometer.

Supporting Information Available: Crystallographic data; NMR data; and luminescence data. This material is available free of charge via the Internet at http://pubs.acs.org.

IC060403L

(23) Sheldrick, G. M. *SADABS*; University of Göttingen: Göttingen, Germany, 2000.
(24) van der Sluis, P.; Spek, A. L. *Acta Crystallogr.* **1990**, *A46*, 194−201.
(25) Sheldrick, G. M. *SHELXL97*; University of Göttingen: Göttingen, Germany, 1997.